Sheffield Hallam University

Localisation of citrullinated proteins in normal appearing white matter and lesions in the central nervous system in multiple sclerosis

BRADFORD, Claire M., RAMOS, Inês, CROSS, Alison K.
<http://orcid.org/0000-0003-0655-6993>, HADDOCK, Gail
<http://orcid.org/0000-0001-8116-7950>, MCQUAID, Stephen, NICHOLAS,
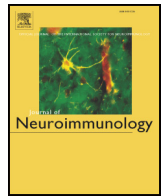Anthony P. and WOODROOFE, M. Nicola <http://orcid.org/0000-0002-8818-
331X>

Citation:

Copyright and re-use policy

Localisation of citrullinated proteins in normal appearing white matter and lesions in the central nervous system in multiple sclerosis

Claire M. Bradford [a],[1], Inês Ramos [a],[2], Alison K. Cross [a], Gail Haddock [a], Stephen McQuaid [b], Anthony P. Nicholas [c], M. Nicola Woodroofe [a],[*]

[a] Biomedical Research Centre, Sheffield Hallam University, Howard Street, S1 1WB South Yorkshire, UK
[b] Neuropathology Laboratory, Department of Pathology, Royal Group of Hospitals Trust, Grosvenor Road, Belfast, Northern Ireland BT12 6BL, UK
[c] Department of Neurology, University of Alabama at Birmingham and Birmingham Veterans Administration Medical Centre, Birmingham, AL 35249-7340, USA

ARTICLE INFO

ABSTRACT

Multiple sclerosis (MS) is a chronic inflammatory neurodegenerative disease, considered to be autoimmune in origin. Post-translational modification of central nervous system proteins, including glial fibrillary acidic protein (GFAP) and myelin basic protein (MBP), through citrullination of arginine residues, may lead to exposure of neoepitopes, triggering autoimmunity. Here we investigated the expression of citrullinated proteins in active MS lesions, MS normal appearing white matter and control brain white matter. We demonstrate increased citrullinated GFAP and MBP by immunohistochemistry and western blotting in areas of ongoing demyelination, suggesting a pivotal role for deimination of GFAP and MBP in MS pathogenesis MS.

© 2014 The Authors. Published by Elsevier B.V. This is an open access article under the CC BY-NC-ND license (http://creativecommons.org/licenses/by-nc-nd/3.0/).

1. Introduction

Multiple sclerosis (MS) is a chronic immune mediated disease of the central nervous system (CNS) affecting approximately 0.1% of Caucasians of north and central European ancestry (Noseworthy et al., 2000), resulting in focal demyelinated lesions or plaques. In general, these lesions are classified as either active or inactive. Active MS lesions are defined by the presence of activated microglia and infiltrating macrophages, which contain remnants of myelin, phagocytosed during the demyelinating process, in addition to large reactive astrocytes (Jack et al., 2005). T cells, B cells and plasma cells are also found in active lesions (Frischer et al., 2009). In contrast, inactive lesions consist of demyelinated foci which are sharply defined and hypocellular with no evidence of active demyelination or axonal loss, but instead prominent fibrillary gliosis (Lucchinetti et al., 2005).

There is increasing evidence that citrullination may play an important role in MS pathogenesis (Nicholas et al., 2004; Harauz and Musse, 2007; Musse and Harauz, 2007). Citrullination is a process whereby an arginine residue is converted to the non-standard amino acid citrulline (Beniac et al., 2000), resulting in the loss of a positive charge and an altered secondary and tertiary structure of the protein (Musse et al., 2006; Harauz and Musse, 2007). This post translational modification (PTM) is carried out by a family of five citrullinating enzymes known as peptidylarginine deiminases (PADs), with PAD2 and PAD4 being the most common PADs found in the brain (Rogers et al., 1977; Vossenaar et al., 2003). Excess citrullination has been reported in the CNS in postmortem MS brain tissue (Nicholas et al., 2004; Mastronardi et al., 2006). Previously, using myelin basic protein (MBP) isolated from normal appearing matter (NAWM) from MS patients and controls, and fractionation of the samples by column chromatography, Moscarello et al. found that 18% of MBP was citrullinated in control tissue compared to 45% of MBP in patients with MS (Moscarello et al., 1994). Further studies by the same group found that in Marburg's disease, as much as 90% of MBP is citrullinated (Wood et al., 1996).

Since citrullination alters the charge of the protein, citrullinated MBP becomes partially unfolded and its interaction with phospholipids is weakened, resulting in myelin sheaths that are not as tightly packed as in normal myelin (Wood and Moscarello, 1989; Beniac et al., 2000). Studies have shown that deiminated MBP is more susceptible to proteolytic digestion by myelin associated proteases (Cao et al., 1999; Pritzker et al., 2000; D'Souza and Moscarello, 2006; Musse et al., 2006). This greater surface exposure and increased cleavage of citrullinated protein by proteases would lead to increased release of immunodominant epitopes, which could then sensitize peripheral blood T cells (Musse et al., 2006; Musse and Harauz, 2007). Furthermore, citrullination

appears to be necessary in order to elicit CD4$^+$ T cell responses, suggesting that 'altered-self' epitopes are only presented to T cells when certain arginine residues have been converted to citrulline (Hill et al., 2003; James et al., 2010). Recently Acharya et al. (2012) have proposed a role for citrullination of neuronal proteins, localised in regions of neurodegeneration, in the generation of autoantibodies in Alzheimer's disease.

Using an antibody which recognises all deiminated proteins (F95) it was reported that citrullination of glial fibrillary acidic protein (GFAP) was substantially higher in the NAWM compared with equivalent control brain tissue (Nicholas and Whitaker, 2002; Nicholas et al., 2004, 2005). In addition, presumed chronic inactive lesions were found to be devoid of citrullinated proteins in this study, except within astrocytes surrounding blood vessels (Nicholas et al., 2004). Using F95 antibody these authors also demonstrated that citrullinated proteins were present in both the brain and spinal cord of mice with myelin oligodendrocyte glycoprotein (MOG)-induced experimental autoimmune encephalomyelitis (EAE), and that citrullination was shown to co-localise within MBP positive regions surrounded by GFAP immunoreactive astrocytes, that were also positive for deiminated proteins (Nicholas et al., 2005).

Here, we investigated the immunohistochemical localisation of citrullinated proteins in post mortem brain tissue from MS patients and normal control cases and confirmed the citrullinated proteins present by western blotting as well as expression of PAD2 mRNA in the CNS by quantitative real-time PCR. PAD2 mRNA expression was also examined in in vitro studies of primary human astrocytes, a human foetal microglial cell line and a human brain endothelial cell line. Using these techniques we demonstrated that increased citrullinated GFAP was found in areas of both ongoing demyelination and myelin loss in active and chronic active MS lesions. Interestingly, where there was complete myelin loss, citrullinated proteins were absent. Lower levels of citrullinated proteins were observed in the MS NAWM and control white matter. Western blot analysis of brain tissue from these patients confirmed that in addition to MBP, GFAP was the major citrullinated protein in the CNS, and the amount of citrullination was increased in active disease, suggestive of a role in the pathogenesis of MS.

2. Materials and methods

2.1. Human tissue

Nineteen blocks of snap-frozen autopsy tissue from 12 clinically and neuropathologically confirmed secondary progressive multiple sclerosis (SPMS) cases, together with nine blocks from 6 normal control cases, were obtained from the UK Multiple Sclerosis Society Tissue Bank, Imperial College, London (Table 1). The MS cases included 10 females, mean age 67.7 years (range 37–86) and 2 males, mean age 58.5 years (range 55–62) and contained lesions typical of active and chronic active disease. Brain tissue was received fresh from autopsy with <24 h death-autopsy times for 11 out of 12 MS cases. For each MS case, between 1 and 3 cerebral tissue blocks, including cortical and perivascular areas with white matter demyelination, were examined. All of the patients had a confirmed diagnosis of MS by both histological and clinical criteria. Control and MS blocks were matched for CNS location.

Serial cryostat sections (10 μm) were processed for haematoxylin and eosin (H&E), oil red-O (ORO), and anti-HLA-DR immunohistochemistry to evaluate the general histology and extent of cellular activation within each block. Perivascular inflammation was graded using a four-point scale (negative, +, ++, +++). Lesions with ORO-positive cells throughout and with perivascular cuffing were classified as active lesions. Blocks that contained ORO-negative regions with hypercellular borders, including ORO positive cells, were classified as chronic active lesions, whereas blocks derived from macroscopically normal white matter with the absence of ORO staining or perivascular inflammation and with resting microglia, identified with anti HLA-DR staining, were classified as normal appearing white matter (NAWM).

2.2. Immunohistochemistry

Serial cryostat sections of 19 MS and 9 control tissue blocks were cut and mounted onto poly-L-lysine coated glass slides (polysine™ slides, catalogue number 631-1349, VWR International Ltd., UK), fixed in ice-cold acetone for 10 min and then allowed to air-dry. Sections were

Table 1
Clinical data of controls and multiple sclerosis cases included in this study.

Case number	Age	Gender	Diagnosis	Total disease duration (years)	Lesion type
MS1	72	Female	SPMS	41	Active
					Chronic active
MS2	73	Female	SPMS	43	Active
MS3	77	Female	SPMS		Chronic inactive
					Chronic active
					Chronic active
					Active
MS4	51	Female	SPMS	21	Chronic active
					Active
					Chronic active
					Chronic inactive
MS5	55	Male	SPMS	43	NAWM
					Chronic active
MS6	86	Female	SPMS	36	NAWM
MS7	78	Female	SPMS	42	NAWM
MS8	71	Female	SPMS	35	Chronic active
MS9	62	Male	SPMS	39	Chronic active
MS10	37	Female	SPMS	17	Chronic active
					Chronic active
					Chronic active
MS11	77	Female	SPMS	21	NAWM
					NAWM
MS12	55	Female	SPMS	25	Chronic active
C1	64	Male	Normal	–	–
C2	69	Female	Normal	–	–
C3	35	Male	Normal	–	–
C4	78	Female	Normal	–	–
C5	60	Female	Normal	–	–
C6	75	Male	Normal	–	–

(−) not applicable.

treated with 5% goat serum with 1% bovine serum albumin (BSA) in phosphate buffered saline (PBS) for 30 min at room temperature (RT), to prevent non-specific binding of the primary and secondary antibodies. Tables 2 and 3 provide a summary of the details of the primary and secondary antibodies and the dilutions used in this study. Following this, sections were incubated with the primary antibody diluted in 0.3% goat serum with PBS overnight at 4 °C, washed in PBS and incubated in the appropriate secondary antibody at 1:500 in 1% BSA with PBS for 1 h at room temperature (RT). Cell nuclei were counterstained with diamidino-2-phenylindole (DAPI), which was included in the mountant (Vector Laboratories, UK). Isotype control primary antibodies were used routinely to assess non-specific binding.

To determine the cellular localisation of peptidyl-citrulline moieties, the following dual-label immunofluorescence protocol was performed. Briefly, sections were co-incubated with both a monoclonal and polyclonal antibody overnight at 4 °C and then detected by co-incubating the appropriate secondary antibodies against mouse and rabbit immunoglobulins (final dilution 1:500) for 1 h at RT. Secondary antibodies were conjugated with fluorescent tags so that immunolabelled structures either appeared green (Alexa 488) or red (Alexa 568). Following three 5 min washes in PBS, sections were placed in 1% Sudan black B for 5 min to block autofluorescence, followed by 8–10 washes in PBS and then mounted as described above. Dual immunofluorescence was performed with polyclonal antibodies against GFAP for the identification of astrocytes and mouse IgM against citrullinated proteins (F95) (Nicholas and Whitaker, 2002). Single staining was also performed using mouse monoclonal antibodies against HLA-DR, a marker for activated macrophages, and myelin oligodendrocyte glycoprotein (MOG) to assess myelin loss.

Prior to carrying out dual immunostaining, serial sections were single-labelled with each mouse or rabbit primary antibody followed by secondary antibodies to anti-rabbit IgG and anti-mouse IgG or IgM respectively to ensure that no cross-reactivity was observed between the primary antibody and the inappropriate secondary antibody. Omission of either primary antibody from the protocol, whilst retaining the secondary antibody was performed to ensure the absence of non-specific binding from the secondary antibody.

2.3. Semi-quantification of citrullination immunoreactivity

Sections of MS and control white matter were anonymised by a third party coding and then regions of interest within sections (lesion, NAWM or control white matter) were scored by two independent blinded observers. Single-label immunostaining for F95 on these sections was graded on a four-point scale: sections displaying low level punctate F95 were graded +, sections showing slightly more elongated fibre staining were ++, whilst more intensive staining was scored +++ and sections with extensive F95 staining were graded ++++ (Fig. 1).

2.4. Confocal scanning laser microscopy

All immunofluorescence images were captured using a Zeiss 510 CSLM inverted confocal, equipped with a krypton/argon laser. Fluorophores were excited at wavelengths of 488 or 568 nm. Co-localisation studies of the dual-labelled samples utilised the co-localisation software available with the Zeiss 510 CSLM. Individual

pixels were scanned for each channel within set intensity thresholds. Co-localised pixels were represented as yellow in the composite image.

2.5. RNA and protein extraction

RNA was isolated from homogenised CNS tissue (2 × 30 μm serial sections) collected from 12 MS and 6 control blocks, as used for immunohistochemistry (Table 1) or cell cultures using TRI-reagent (Sigma, UK). Briefly, either tissue or cells were homogenised in 1 ml TRI-reagent, followed by vortex mixing and centrifugation at 12,000 g for 15 min at 4 °C to remove lipids. The supernatant was transferred to clean microcentrifuge tubes, and RNA and protein were extracted following the manufacturer's instructions (Sigma, UK). RNA quality was checked on 1% agarose gels. Protein concentrations were determined by the bicinchoninic acid assay (Sigma, UK).

2.6. Quantitative real time PCR

Samples (1 μl) of total RNA were reverse transcribed to cDNA using Superscript II reverse transcriptase (Invitrogen, UK). Negative controls were run in parallel without either superscript II or RNA, to ensure that there was no genomic DNA or RNA contamination. Using the fluorescent TaqMan 5′ nuclease assay (Applied Biosystems, UK) each cDNA sample was analysed for the expression of PAD2, PAD4 and housekeeping genes cyclophilin A and hypoxanthine-guanine phosphoribosyltransferase-1 (HPRT1) (Applied Biosystems, assay numbers Hs00247108_ml, Hs012387.2_ml, Hs99999904_ml and Hs99999909_ml, respectively) by qRT-PCR. Each 10 μl reaction consisted of 2× TaqMan Universal PCR Master Mix (Applied Biosystems, UK), 1 μl primer and FAM labelled probe and 1 μl of template cDNA. Each primer and probe set was designed by Applied Biosystems (UK) and selected on the basis that they crossed exon–exon boundaries to prohibit any amplification of contaminating genomic DNA. Reactions were carried out in a 96-well reaction plate (Applied Biosystems, UK) using the Applied Biosystems 7900HT fast real-time PCR system. The thermal profile of the reaction was as follows: 50 °C for 2 min, 95 °C for 2 min, and 40 cycles of denaturation at 95 °C for 15 s and annealing/extension at 60 °C for 1 min. Emitted fluorescence was measured in real-time and later used to construct an amplification plot using ABI Prism 7900HT Sequence Detection System software version 2.2.1. Relative mRNA levels of the above genes were determined using the cycle threshold (CT) and the $2^{-\Delta CT}$ method. The expression of PAD2 was normalised against expression of the housekeeping genes cyclophilin A and HPRT1. The relative mRNA levels of PAD2 were determined using the formula $2^{-\Delta CT}$ where $\Delta CT = CT$ (target gene) $- CT$ (average cyclophilin A and HPRT1). These experiments were carried out in duplicate, independently.

Table 3
Secondary antibodies used for immunohistochemistry.

Immunogen	Species	Conjugate	Dilution	Source (catalogue number)
Mouse IgM	Goat	Alexa 488	1:500	Invitrogen (A-21042)
Mouse IgG	Goat	Alexa 568	1:500	Invitrogen (A-11004)
Rabbit IgG	Goat	Alexa 568	1:500	Invitrogen (A-11011)

Table 2
Primary antibodies used for immunohistochemistry.

| Primary antibody	Antibody type	Target	Source	Dilution
F95	Mouse monoclonal	Citrullinated proteins	Anthony Nicholas, USA	1 in 500
HLA-DR	Mouse monoclonal IgG2b	Activated macrophages and microglia	Novocastra, Newcastle upon Tyne, UK. (Catalogue number: NCL-LN3)	1 in 50
MOG	Mouse monoclonal	Myelin	Richard Reynolds, London, UK	1 in 100
GFAP	Rabbit polyclonal IgG	Astrocytes	Abcam, Cambridge, UK. (Catalogue number: ab7260)	1 in 1000
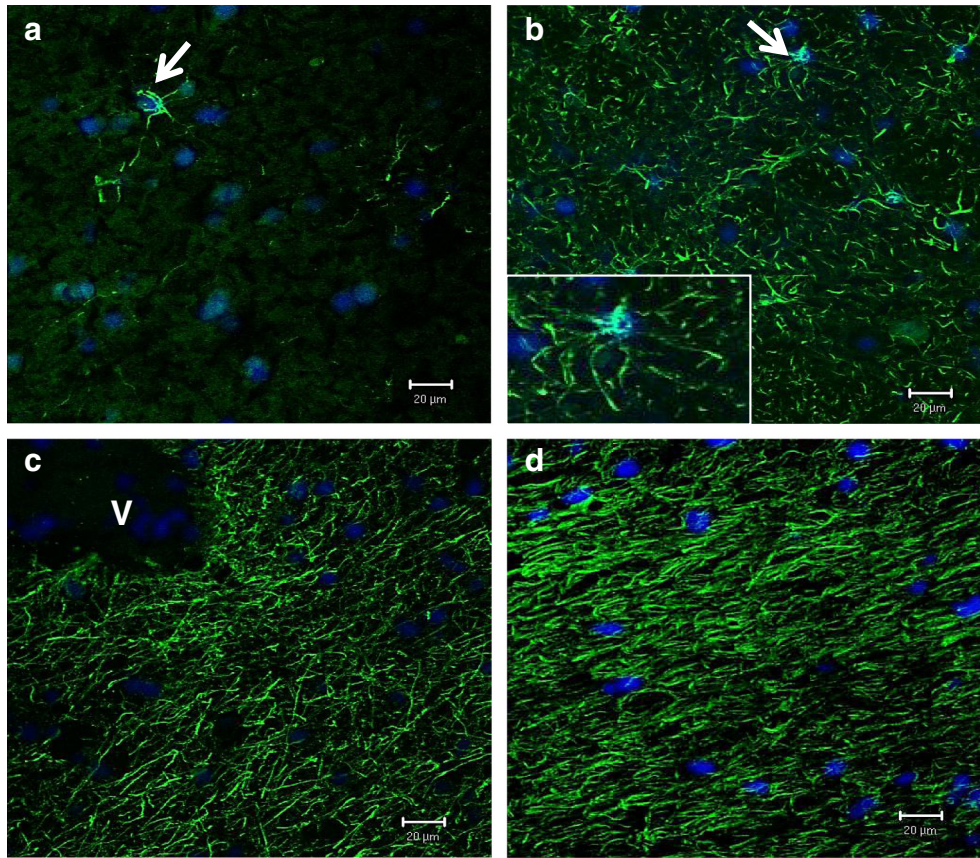
Fig. 1. Scoring of citrullinated protein (pep cit) staining in control (C2), MS NAWM (MS9) and lesion (MS4) by immunofluorescence and confocal microscopy. Levels of staining were graded (a) 1+, single astrocytes were stained (arrow) (b) 2+, levels of staining became more diffuse but astrocyte bodies are still visible (arrow and inset at higher magnification), (c) 3+, staining is more dense and filamentous. Blood vessel lumen (V) and (d) 4+, widespread filamentous staining is seen together with an increase in intensity of staining. Nuclei are stained blue (DAPI).

2.7. Western blotting

Extracted protein samples (30 μg) were loaded into wells and separated by SDS-polyacrylamide gel electrophoresis on 12% pre cast gels (Invitrogen, Paisley, UK) at 150 V for 90 min. Proteins were transferred onto nitrocellulose membranes (Hybond-C, GE Healthcare Life Sciences, Amersham, UK) at 100 V for 1 h. Membranes were blocked for 90 min in 5% BSA in Tris-buffered saline (TBS) containing 0.02% Tween-20 solution (TBS–Tween). Membranes were then washed three times in TBS–Tween and incubated in primary antibody (F95 1:1000, anti GFAP 1:1000 or anti β-actin 1:1000) overnight at 4 °C. The following day, membranes were incubated with secondary antibody (labelled with Alexa 680 or IR800) for 1 h at RT, then washed twice in TBS–Tween and once in TBS. Signal intensities were then analysed using the LiCOR Odyssey infrared image system (Li-COR Biosciences Cambridge, UK Ltd.) ensuring that each channel was set at the same exposure time between patient samples.

2.8. SDS-PAGE, in-gel digestion and extraction of peptides from MS brain tissue

MS tissue protein extract (from MS4) which had shown the most extensive citrullination by immunohistochemical and western blot analysis (30 μg) and pure MBP (10 μg) (Sigma, UK), as a positive control, were fractionated on pre-cast 10% NuPage Novex Bis-Tris gels (Invitrogen, UK) using SDS-PAGE. Following SDS-PAGE, the gel was stained using Instant Blue (Expedeon, UK) according to the manufacturer's protocol. Protein bands of interest were then excised from the gel using a sterile blade and placed in microcentrifuge tubes.

Following this, gel pieces underwent alkylation and reduction followed by extraction of peptides. Briefly, each gel piece was rehydrated in 40 μl 10 mM dithiothreitol, vortexed followed by pulse-centrifugation, and then incubated on a heat block at 56 °C for 45 min. The supernatant was then removed and 40 μl 55 mM iodoacetamide was added to each gel piece, vortexed followed by pulse-centrifugation. The sample was then left in the dark for 30 min to allow the reaction to proceed. The supernatant was then discarded and the gel piece was washed in 100 μl 25 mM Tris-HCL (pH 9.3), vortexed for 10 min followed by pulse-centrifugation. The supernatant was then removed and 200 μl 100% acetonitrile (ACN) was added to the gel piece for ~10 min. The supernatant was removed and subjected to Speed Vac until gel pieces were dry. 25 μl (10 μg/ml) Lys C solution (Promega, UK) was added to each gel piece and samples were allowed to rehydrate for 1 h on ice. The excess Lys C solution was then removed and the gel piece was covered with ~40 μl 25 mM Tris–HCl (pH 9.3). The gel pieces were then incubated on a shaker overnight at 37 °C. Following this, gel pieces were subjected to pulse-centrifugation, followed by removal of the supernatant into a clean microcentrifuge tube. 30 μl 50% ACN 0.1% trifluoroacetic acid (TFA) was added to each gel piece, vortexed for 15 min and then subjected to pulse-centrifugation. The supernatant was removed and added to the supernatant from the previous step. This was then repeated. The resulting extract was then subjected to Speed Vac centrifuge to reduce the sample volume to ~10 μl. To concentrate and purify samples, Zip Tips® (Millipore, UK) were used prior to spotting samples onto the target plate and were used according to the manufacturer's instructions. Following this 0.5 μl α-cyano-4-hydroxylcinnamic acid and aniline in ACN: water: TFA (1:1:0.1 by volume) was spotted directly onto the target plate (10 mg/ml) followed by 0.5 μl sample.
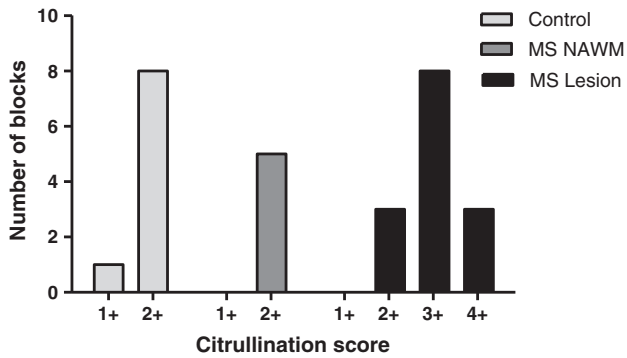
Fig. 2. Levels of citrullinated protein scored in each tissue block used in this study. Control white matter (n = 9), MS NAWM (n = 5) and lesions from MS cases (n = 14). Anonymised blocks were blindly graded by two independent researchers. Any discrepancies between blocks were reviewed again and a consensus agreement reached between the two raters. Levels of citrullinated proteins were highest in MS lesions compared to control white matter and MS NAWM, with control white matter and MS NAWM displaying similar low levels of deiminated proteins.

2.9. Matrix-assisted laser desorption ionisation ion mobility separation tandem mass spectrometry (MALDI-IMS-MS/MS)

MALDI IMS–MS/MS was performed using a HDMS SYNAPT™ G2 system (Waters Corporation, UK). The instrument was used in positive ionisation mode. In order to achieve good quality MS/MS spectra, spectra were acquired by manually moving the laser position and adjusting the collision energy to achieve good signal to noise for product ions across the full m/z range of the spectrum. Collision energies were adjusted from 70 to 100 eV during acquisition and acquisition times were generally 5–10 s per spectrum. The resulting peaks obtained from the MS/MS spectra were uploaded in a text file format to perform a Mascot (Matrix Science, UK) search which used the UniProt database in order to generate a sequence match. Searches were performed for Lys C specificity and two missed cleavages were allowed. Mass deviations for precursor ions and for fragment ions were set at 10 ppm and 0.75 Da, respectively.

2.10. Cell culture

Primary adult human astrocytes isolated from either CNS NAWM obtained at autopsy from UK MS Society Tissue Bank (UKMSTB; donor labelled MS16) or from temporal lobectomy resections for treatment of epilepsy at King's College Hospital (KCH, London; donor labelled EP15) (a kind gift from Dr I. Romero, Open University UK) were cultured in astrocyte medium composed of 1:1 nutrient mixture of MEM-α and F-10, supplemented with fungizone (250 units/ml), penicillin (100 units/ml), streptomycin (50 μg/ml), 10% heat inactivated FCS (Invitrogen, UK) and 1% human AB serum (Sigma, UK). The microglial cell line, CHME-3 (a kind gift from Prof M. Tardieu, Universite Paris Sud, France), was cultured in Dulbecco's modified Eagle's medium (Sigma, UK), supplemented with 10% foetal calf serum (FCS) (Invitrogen, UK) and 2 mM Ala-Gln solution (Sigma, UK). The human adult brain endothelial cell line, hCMEC/D3 (Weksler et al., 2005), was cultured on collagen type I from rat tail (Millipore, UK) in the commercially
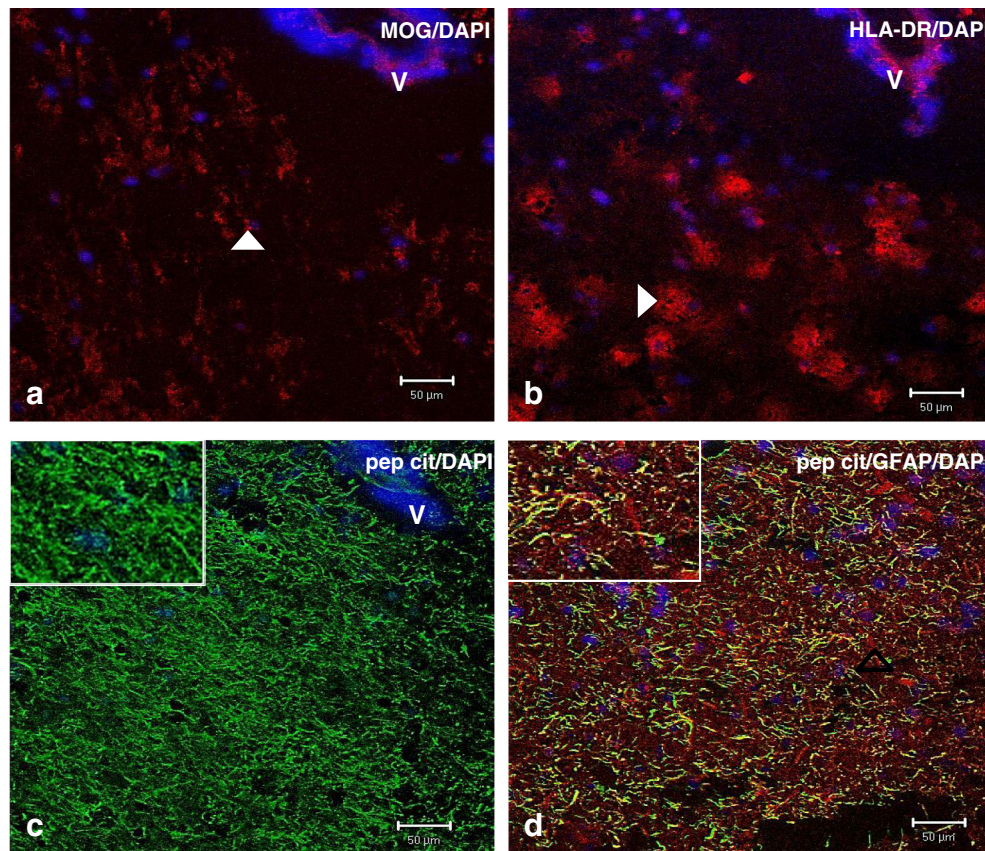

Fig. 3. An actively demyelinating MS lesion (MS2) visualised using single and dual staining immunofluorescence microscopy of serial tissue sections. (a) Ongoing demyelination evidenced by disrupted, intermittent MOG staining (red), indicated by arrow head, (b) Activated HLA-DR + (red) foamy macrophages, indicated with arrow head, (c) Strong, extensive immunoreactive staining for citrullination with F95 antibody (green), (d) Citrullination (green) was predominantly co-localised (yellow) to astrocytes (GFAP; red) within the demyelinating lesion, although not all astrocytes were double positive, arrow head indicates single stained GFAP + astrocytes. V indicates the location of a blood vessel seen in serial sections in a–c. Nuclei are stained blue (DAPI).

available complete media EGM™-2 (endothelial growth medium) supplemented with hydrocortisone, vascular endothelial growth factor, gentamycin, ascorbic acid, human endothelial growth factor, long R insulin-GF, heparin, human FGF-β (Lonza, UK), with penicillin (50 units/ml), streptomycin (50 μg/ml) and 2% heat inactivated FCS (Invitrogen, UK). The cells were maintained at 37 °C with 5% CO_2/95% air in a humidified environment.

2.11. Statistical analysis

For qRT-PCR data, statistical significance was displayed as mean ± SEM. The probability of statistical differences in PAD2 mRNA expression between control white matter, MS NAWM and MS lesional tissue was determined by Kruskal–Wallis followed by Conover–Inman. The probability of statistical differences in PAD2 mRNA expression between MS16, EP15, CHME3 and hCMEC/D3 was determined by Kruskal–Wallis followed by Conover–Inman. Statistical differences were considered significant at $* p < 0.05$, $**p < 0.01$ and $***p < 0.001$.

3. Results

3.1. Citrullination is increased in areas of ongoing demyelination in active and chronic active lesions

Expression of citrullinated proteins within regions of interest on individual sections was graded from 1 + to 4 + (Fig. 1). Intense immunoreactivity for citrullinated proteins was seen in both active and chronic active lesions of MS tissue blocks, as compared to NAWM in MS and control white matter tissue. The highest levels of citrullination (3 + and 4 +) were observed in lesions, whereas both control and NAWM samples were rated 2 + except for one control case which was graded 1 + (Fig. 2). In control and NAWM astrocytes were identifiable by their morphology as being positively stained for citrullinated peptides (Fig. 1a, b) whereas MS tissue which was categorised as being 3 + or 4 + had such extensive staining that it was difficult to discern individual cell bodies (Fig. 1c, d). Strong peptidyl-citrulline immunoreactivity was observed in active lesions with ongoing demyelination, evidenced by thinning of the myelin sheath, shown by disrupted MOG staining, and was associated with areas of activated HLA-DR + foamy macrophages/microglia (Fig. 3a–c). Where myelin staining was absent within lesion centres, there was very little evidence of citrullinated proteins (Fig. 4a–c), although activated HLA-DR + macrophages were present, these did not have a foamy appearance indicating that myelination was not ongoing. Using dual label immunofluorescence for peptidyl-citrulline and GFAP, the intensity of GFAP staining was markedly increased in active MS lesions, and was predominantly colocalised with F95 immunoreactivity (Fig. 3d). In chronic active lesions, citrullination of protein can be seen at the edge of the advancing demyelination and advancing into the NAWM (Fig. 4d). NAWM from MS specimens showed weak peptidyl-citrulline immunoreactivity, with immunoreactivity within GFAP positive astrocytes, observed at the abluminal region of blood vessels in the glia limitans (Fig. 5a–d). Control white matter also showed areas with sparse peptidyl-citrulline immunoreactivity, with the strongest staining at the glia limitans and primarily associated with GFAP immunoreactivity (Fig. 6a–d). Myelin was intact and normal in these cases, with resting microglia (Figs. 5b, 6b).
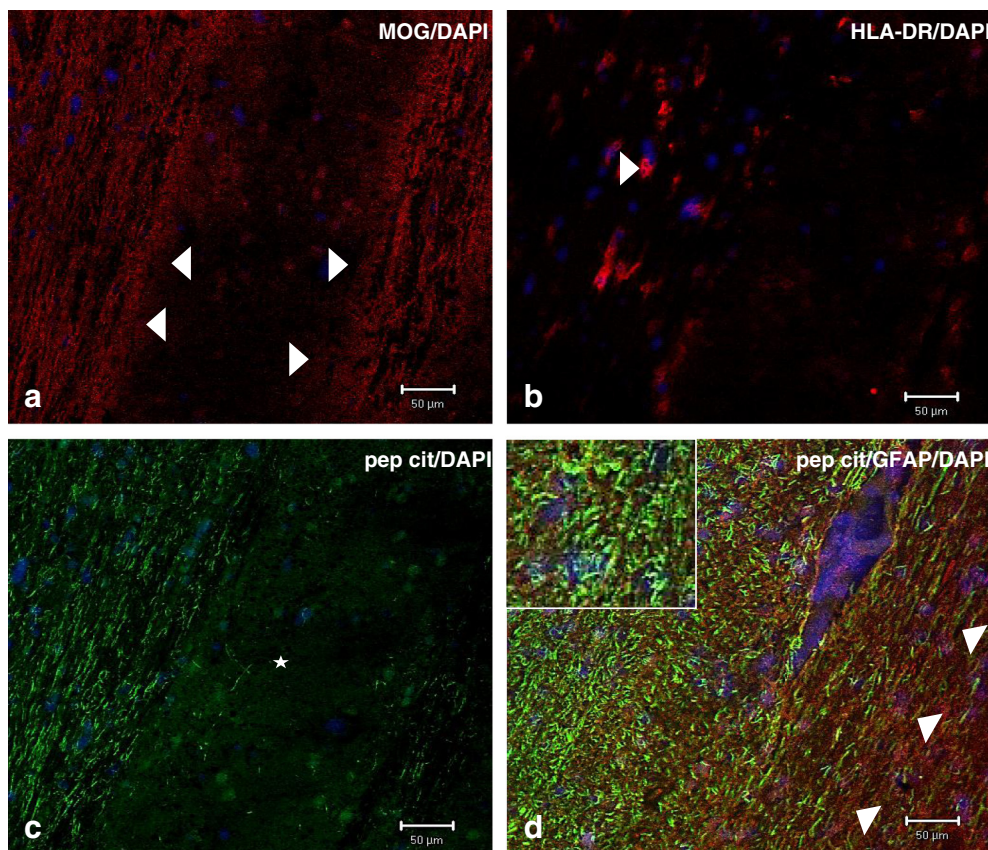

Fig. 4. An active demyelinated MS lesion (MS4) visualised using single and dual staining immunofluorescence of serial tissue sections. (a) MOG staining (red) indicates loss of myelin with the borders of the lesion indicated with arrow heads. (b) Activated HLA-DR + microglia (red), arrow head and (c) strong immunoreactive staining for citrullination in areas where myelin is intact. In the central area with complete myelin loss, indicated by * there was an absence of citrullinated proteins. (d) Citrullination (green) was co-localised (yellow) to astrocytes (GFAP; red); plaque border is indicated with arrow heads. Nuclei are stained blue (DAPI).
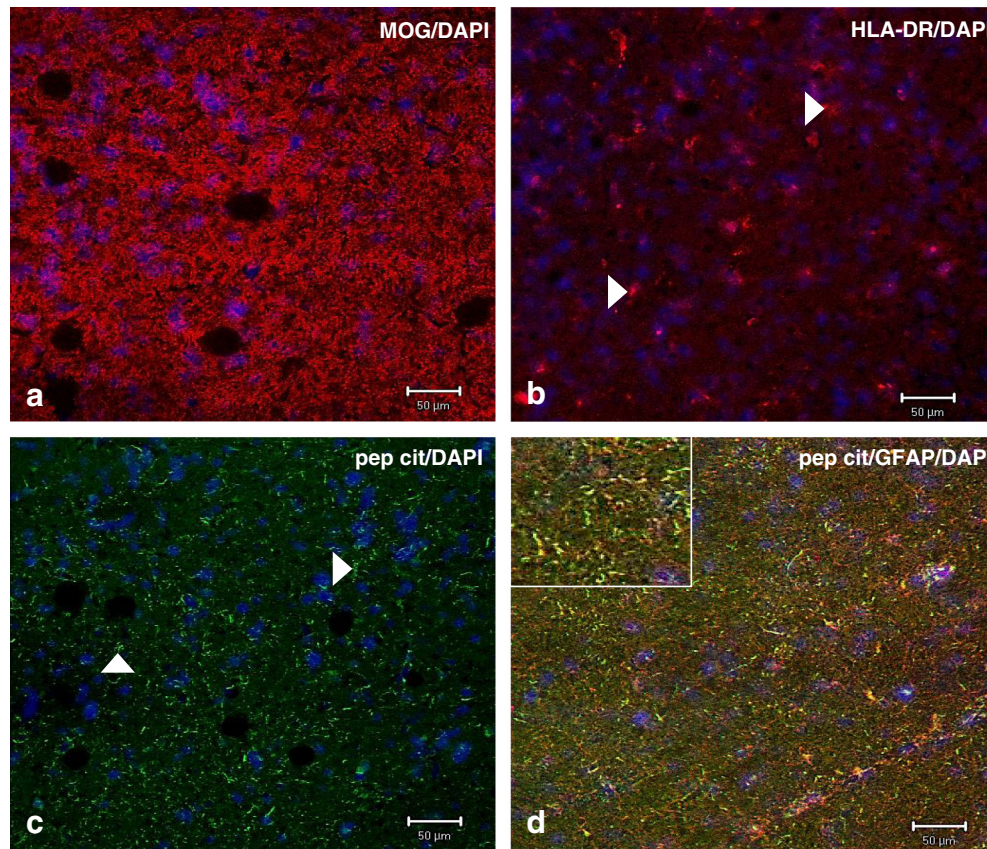
Fig. 5. Citrullination in MS NAWM (MS7) visualised using single and dual staining immunofluorescence of serial sections. (a) Intact myelin stained for MOG (red), (b) Resting, weakly HLA-DR+ microglia (red) (arrow heads), (c) weak immunoreactive staining for citrullination (F95, green) (arrow heads) which was predominantly (d) co-localised (yellow) to astrocytes (GFAP; red). Nuclei are stained blue (DAPI).

3.2. PAD2 mRNA was constitutively expressed in control, NAWM and MS lesion tissue blocks

PAD2 was expressed at the mRNA level in control white matter, MS NAWM and MS lesion brain tissue (Fig. 7). There was significantly less PAD2 mRNA in the MS NAWM compared to both control white matter and MS lesional brain tissue. PAD4 mRNA was expressed at similar levels within control, NAWM and lesional brain tissue and the relative expression was ~100 fold lower than that for PAD2 mRNA (data not shown).

3.3. Western blot analysis of citrullinated proteins in human brain tissue

Western blot analysis of proteins extracted from control white matter, MS lesions and NAWM all showed multiple bands of citrullinated proteins using the F95 antibody (Fig. 8a). In control white matter, MS NAWM and MS lesions, seven major bands were detected with F95 antibody, including one at the expected 50 kDa molecular mass for GFAP and one at 18.5 kDa suggestive of citrullinated MBP (Fig. 8a). Further unidentified bands were seen at 250, 75, 15 and 10 kDa. Two bands at ~48 and ~50 kDa were most prominent, which were positively identified as citrullinated GFAP isoforms by dual labelling of the blots with both antibodies (F95 and anti GFAP) (Fig. 8c).

3.4. MALDI IMS–MS/MS of peptides extracted from an MS lesion

A number of MBP and GFAP peptides were positively identified from in-gel digests of protein bands corresponding to citrullinated proteins extracted from an MS case and subsequent MALDIIMS–MS/MS

(Table 4). Protein bands visualised at ~15 and ~18.5 kDa on a western blot were confirmed as MBP, whereas protein bands visualised at ~48 and 50 kDa were confirmed as GFAP. The remaining bands visualised at 250, 75, 15 and 10 kDa were not identified by MALDIIMS–MS/MS.

3.5. PAD2 gene expression in cells of the CNS

Real-time PCR analysis of all three cell types, primary human astrocytes (MS16 and EP15), a human foetal microglial cell line (CHME3) and human brain endothelial cell line (hCMEC/D3), showed constitutive expression of PAD2 mRNA (Fig. 9).

4. Discussion

This study shows for the first time that high levels of citrullinated proteins were localised in areas of activated macrophages with ongoing demyelination and myelin thinning. In comparison, much lower levels of citrullination were consistently found in the NAWM of MS and control white matter tissue where there was no demyelination. This suggests that the process of citrullination is intimately linked with that of demyelination, the major hallmark of MS. Another striking finding was that the increased expression of citrullinated proteins was primarily colocalised with GFAP in both active and chronic active lesions in brain tissue taken from patients with MS. These findings could represent an increase in the amount of naturally occurring citrullinated GFAP overall in MS, or more arginine residues in GFAP may be citrullinated in the disease state. In previous studies of MBP, the number of citrulline moieties was increased in more severe disease (Wood et al., 1996).
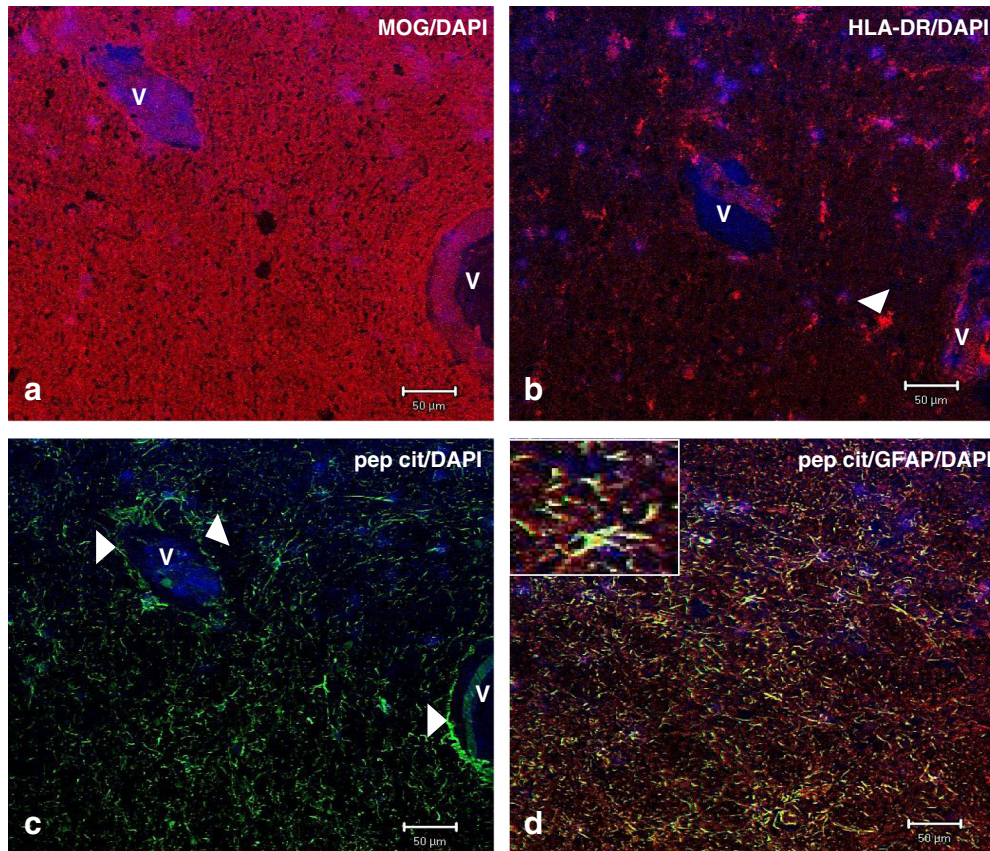
Fig. 6. Citrullination in control white matter (C5) visualised using single and dual staining immunofluorescence of serial tissue sections. (a) Intact myelin stained for MOG (red) throughout. (b) Low level of resting weakly HLA-DR+ microglia (arrow head). (c) Weak immunoreactive staining for citrullination (F95, green) which was predominantly (d) co-localised (yellow) to astrocytes (GFAP; red) and was particularly prominent at the *glia limitans* surrounding blood vessels (V) (arrow heads). Nuclei are stained blue (DAPI).

Due to increasing evidence indicating that non-lesional NAWM in MS patients has underlying pathology (Nicholas et al., 2004; Kutzelnigg et al., 2005; Frischer et al., 2009; van der Valk and Amor, 2009), the NAWM was also examined for the presence of citrullinated proteins. However, in this study we were unable to identify a difference in the levels of citrullination between control white matter and MS NAWM compared to MS lesional brain tissue. This finding was unexpected, as previously Nicholas et al. (2004), using three control and three MS blocks, were able to show increased expression of citrullinated GFAP in the NAWM of brain tissue taken from patients
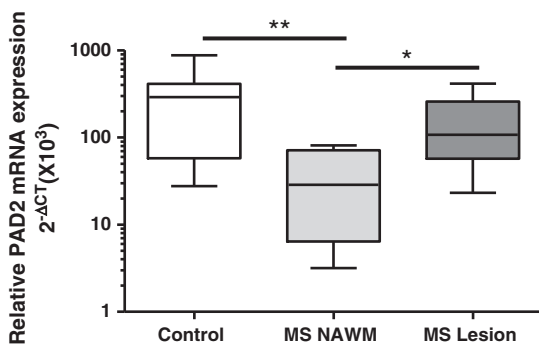
with SPMS; however, these tissue specimens were taken primarily from patients with more inactive disease (Nicholas et al., 2004). In contrast, our study examined MS brains containing both active and chronic active plaques as opposed to NAWM, which may account for this difference. In addition, in the current study, additional markers were used to assess the pathology of the lesion and surrounding NAWM, most importantly lymphocyte and monocyte infiltration, extent of microglia activation and myelin thinning and loss.

Western blotting showed the presence of multiple citrullinated proteins, with bands at ~48 and ~50 kDa, identified as GFAP isoforms and a band at 18.5 kDa identified as MBP (Harauz et al., 2004; Boggs, 2006; Ferguson et al., 2009). Additional bands of citrullinated proteins were observed at 250, 75, 15 and 10 kDa, and although the 75 kDa band was previously detected in NAWM from MS cases (Nicholas et al., 2004), further work to identify these proteins through matrix assisted laser desorption ionisation mass spectrometry and tandem mass spectrometry is needed.

We were able to show PAD2 mRNA expression in control white matter, MS NAWM and lesion tissue as well as in cell culture in brain endothelial cells, microglia and astrocytes. Interestingly, there was significantly less PAD2 mRNA in the MS NAWM compared to both control white matter and MS lesional brain tissue. Although these results are unexpected, the mRNA level of PAD2 does not necessarily reflect the protein expression or activity of the enzyme. PAD2 mRNA expression in microglia and astrocytes was predicted as previous immunocytochemical studies have shown the expression of PAD2 in glial cells (Akiyama et al., 1990), in particular microglia (Vincent et al., 1992; Asaga et al., 2002; Asaga and Ishigami, 2007) and astrocytes (Vincent et al., 1992; Asaga and Senshu, 1993; Asaga and Ishigami,

Fig. 7. qRT-PCR analyses showing PAD2 mRNA expression in control white matter (control, n = 9), MS NAWM (NAWM, n = 5) and lesions from MS cases (MS lesion, n = 14) (Log scale). qRT-PCR data was calculated using the Comparative Quantitation ΔCT method. Significant differences between control white matter, MS NAWM and MS lesion tissue are marked by asterisks (*p < 0.05, **p < 0.01).

a) pep cit   b) GFAP
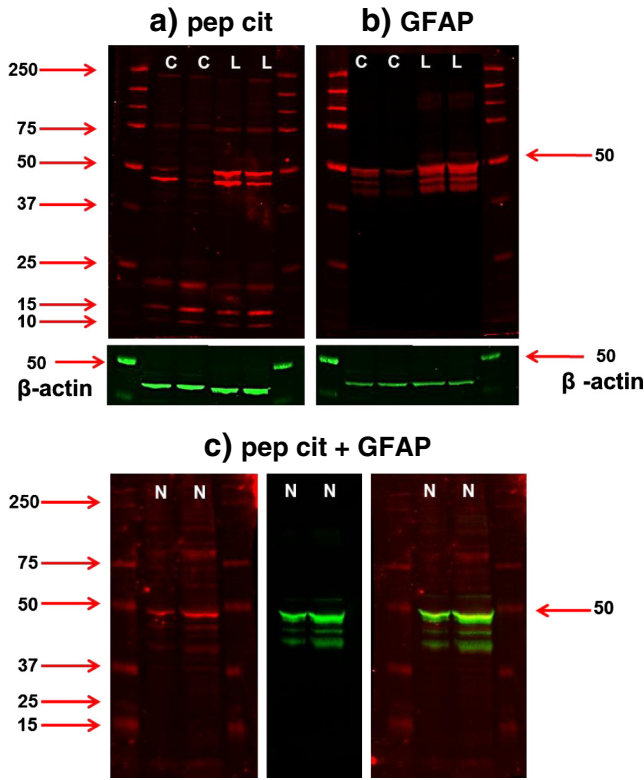

c) pep cit + GFAP

Fig. 8. Western blot analysis of proteins extracted from control white matter (C), MS NAWM (N) and MS lesional (L) brain tissue for (a) peptidyl-citrulline (red), (b) GFAP (green) and (c) peptidyl-citrulline (red) co-localised (yellow) with GFAP (green). Multiple bands of citrullinated proteins were shown, with two of those bands identified as citrullinated GFAP isoforms. The third band of lower MW for GFAP is not citrullinated. The first and last lanes represent standard molecular weight markers, with β-actin antibody used as a loading control (green).

Fig. 9. Basal expression of PAD2 mRNA in different preparations of primary human astrocytes, a human foetal microglial cell line (CHME3) and a human brain endothelial cell line (hCMEC/D3). Data presented as the mean ± SEM. Significant difference between MS16 and other cells tested is indicated, *** $p < 0.001$ (Kruskal–Wallis with Conover-Inman, n = 21).

2000; Asaga et al., 2001; Acharya et al., 2012). This is the first study to show the expression of PAD2 mRNA in brain endothelial cells. PAD4 mRNA, although previously described in human brain, was detectable by qPCR in this current study at very low levels, and PAD4 mRNA was present at similar low levels in control, NAWM and lesional tissue and thus it is likely that the citrullinated proteins present in MS tissue described here are as a result of the activity of PAD2, which has previously been reported as the predominant isoform found in the CNS (Jin et al., 2013).

Numerous studies have identified citrullination of MBP in MS, but this is the first study that has shown directly that high levels of citrullination are associated with areas of ongoing demyelination. When myelin loss is complete, in the centre of chronic active lesions,
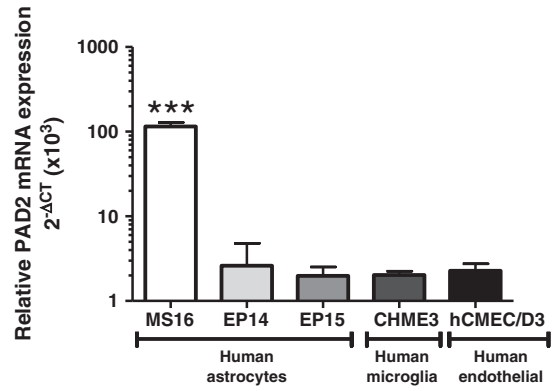
citrullinated proteins are no longer detectable by immunohistochemistry. Our findings provide evidence that citrullination of MBP precedes the actual loss of myelin, indicating that this modified myelin, with citrullinated MBP, is more susceptible to demyelination due to the decreased compaction of the lipid bilayers and increased exposure of proteins, which can trigger an immune response directed at myelin. Previously, using MBP isolated from NAWM of patients with MS and controls, and fractionation of the samples by column chromatography, Moscarello et al. (1994) found that 18% of MBP was citrullinated in control tissue compared to 45% of MBP in patients with MS. Further studies by the same group found that in Marburg's disease, as much as 90% of MBP is citrullinated (Wood et al., 1996) and contained 18 citrulline residues and only 1 arginine residue compared with 6 citrulline and 13 arginine residues in MBP from control and MS cases (Wood et al., 1996). A number of studies have shown that deiminated MBP is unable to compact lipid bilayers, causing membrane destabilisation, thereby, possibly promoting demyelination (Brady et al., 1981; Wood and Moscarello, 1989; Boggs et al., 1999; Beniac et al., 2000). In addition, deiminated MBP is more susceptible to proteolytic digestion by myelin-associated proteases (Cao et al., 1999; Pritzker et al., 2000; D'Souza and Moscarello, 2006; Musse et al., 2006). This greater surface exposure and greater cleavage of the citrullinated protein by enzymes would lead to increased release of the immunodominant epitope, which could then prime microglia in the CNS and sensitize peripheral blood T cells (Musse et al., 2006; Musse and Harauz, 2007).

GFAP is the main intermediate filament protein in mature astrocytes and is involved in a number of structural and functional processes, including proliferation, vesicle trafficking, autophagy and synaptic interactions with neurons as well as contributing to the *glia limitans* at

Table 4
List of peptides identified using MALDI-IMS–MS/MS and Mascot.

Protein	Accession number	Mass (Da)	Observed m/z with MALDI/MS	Amino acid sequence	Protein score	Mascot threshold score at 95% significance
GFAP	P1436	49.880	1161.6376	VRFLEQQNK	32	>19
			1161.6392	VRFLEQQNK	31	>18
			1297.7561	ALAAELNQLRAK	76	>13
			1297.7612	ALAAELNQLRAK	72	>13
			1297.7612	ALAAELNQLRAK	72	>13
			1405.8020	LALDIEIATYRK	44	>12
			2074.1060	FADLTDAAARNAELLRQAK	65	>16
			2102.0259	DEMARHLQEYQDLLNVK	62	>13
MBP	P02686	33.117	1491.8308	NIVTPRTPPPSQGK	51	>17
			1491.8317	NIVTPRTPPPSQGK	38	>16
			1897.9371	SHGRTQDENPVVHFFK	76	>15

Following MS/MS a peptide peak list consisting of peptide mass values was exported into Mascot where peptide identification was performed, resulting in protein identification including the peptide amino acid sequence, score and Mascot threshold score. A protein score of ≥30 is considered a good score if two or more peptides are identified within the same sample. Individual ions scores of >16 indicate identity or extensive homology ($p < 0.05$) (Mascot threshold score at 95% significance).

blood vessels in the CNS (Middeldorp and Hol, 2011). GFAP is also thought to play an important role in astrocyte motility, with motility of GFAP−/− astrocytes shown to be greatly reduced compared to GFAP-expressing astrocytes (Lepekhin et al., 2001). Vesicle trafficking has also been shown to be reduced in astrocytes from mice with double knock-outs of GFAP and vimentin (Potokar et al., 2007, 2008). Neuronal activity is closely linked to the release and uptake of the neurotransmitter glutamate, which requires the interaction between astrocytes and neurons (Pines et al., 1992; Storck et al., 1992; Rothstein et al., 1994). GFAP plays a key role in modulating astrocytic glutamate transporter trafficking and function and in the control of glutamine production. GFAP is subjected to multiple post-translational modifications that have important consequences for its structure and functions (Middeldorp and Hol, 2011). Whilst the exact function of citrullination of GFAP in astrocytes is currently unknown, it may have detrimental effects on a number of physiological processes, such as reducing astrocyte motility and vesicle trafficking, preventing the phosphorylation of GFAP during cell proliferation (Inagaki et al., 1994), or affecting the ability of astrocytes to effectively remove glutamate from the extracellular environment leading to neuronal glutamate excitotoxicity, that may contribute to pathological processes in MS (Bak et al., 2006). Astrocyte injury has been suggested as an important early step in brain inflammation (Sharma et al., 2010). At present, potential pathological alterations of astrocytes in MS lesions have not received major attention; however, the above studies, as well as previous studies (Nicholas et al., 2004) and the present results showing high levels of citrullinated GFAP in astrocytes in MS lesions, indicates the need for further investigation of alterations of astrocytes in the pathogenesis of this demyelinating disease.

In order for PAD2 to become active, raised intracellular calcium ions must be present. There are many physiological and pathological conditions that could lead to raised intracellular calcium and subsequent activation of PAD2 in both neurons and glia, including hypoxia and excitotoxicity (Sambandam et al., 2004; Shideman et al., 2006; Smith, 2007). Subsequent activation of PAD enzymes, both intracellularly and extracellularly, would lead to increased citrullination of proteins as reported here in areas of macrophage activation. In addition, the PAD2 promoter has been found to be hypomethylated in the white matter of MS cases compared to control subjects (Mastronardi et al., 2007). Recently this hypomethylation of the PAD2 promoter has also been found to occur in peripheral blood mononuclear cells (PBMCs) taken from MS patients and is associated with significant increased peripheral PBMC PAD2 expression in these individuals as compared to controls (Calabrese et al., 2012). Taken together it seems that hypomethylation of the PAD2 promoter could be a principal event in inducing the transcription of PAD2 and subsequent increased activity of the enzyme, through increases in intracellular calcium ions, leading to citrullination of proteins in MS. A recent study has also shown that upon contact with stimulated T cells, the expression of PAD2 is upregulated in human monocytes (Ferrari-Lacraz et al., 2010), which may also be the case in lesions when macrophages come into contact with activated T cells.

Future work will involve investigating factors which increase PAD2 activity in astrocytes in vitro, as this will provide a better understanding of the mechanisms underlying the increased citrullination of GFAP and MBP seen in MS brain. Factors such as hypoxia, known to cause increased cytoplasmic calcium mobilisation from mitochondrial stores and increased glutamate, may alter PAD2 expression in astrocytes (Duchen, 2004; Sambandam et al., 2004; Middeldorp and Hol, 2011).

In summary, the presented data supports the hypothesis that deimination is important in the pathogenesis of MS, both in terms of citrullination of MBP preceding demyelination and citrullination of GFAP and its possible effect(s) on astrocyte function(s). A working hypothesis at present would be that a presently unknown trigger results in the activation of PAD2 by increasing intracellular calcium, which results in the citrullination of MBP and GFAP, in addition to other proteins in the brain. The result is an autoimmune attack against these altered proteins which leads to other detrimental effects on their function, contributing to MS pathogenesis.

Ethical approval

Acknowledgements

Appendix A. Supplementary data

Supplementary data to this article can be found online at http://dx.doi.org/10.1016/j.jneuroim.2014.05.007.

References

Acharya, N.K., Nagele, E.P., Han, M., Coretti, N.J., DeMarshall, C., Kosciuk, M.C., Boulos, P.A., Nagele, R.G., 2012. Neuronal PAD4 expression and protein citrullination: possible role in production of autoantibodies associated with neurodegenerative disease. J. Autoimmun. 38, 369–380.

Akiyama, K., Inoue, K., Senshu, T., 1990. Immunocytochemical demonstration of skeletal muscle type peptidylarginine deiminase in various rat tissues. Cell Biol. Int. Rep. 14, 267–273.

Asaga, H., Ishigami, A., 2000. Protein deimination in the rat brain: generation of citrulline-containing proteins in cerebrum perfused with oxygen-deprived media. Biomed. Res. Tokyo 21, 197–206.

Asaga, H., Ishigami, A., 2007. Microglial expression of peptidylarginine deiminase 2 in the prenatal rat brain. Cell. Mol. Biol. Lett. 12, 536–544.

Asaga, H., Senshu, T., 1993. Combined biochemical and immunocytochemical analyses of postmortem protein deimination in the rat spinal cord. Cell Biol. Int. 17, 525–532.

Asaga, H., Nakashima, K., Senshu, T., Ishigami, A., Yamada, M., 2001. Immunocytochemical localization of peptidylarginine deiminase in human eosinophils and neutrophils. J. Leukoc. Biol. 70, 46–51.

Asaga, H., Akiyama, K., Ohsawa, T., Ishigami, A., 2002. Increased and type II-specific expression of peptidylarginine deiminase in activated microglia but not hyperplastic astrocytes following kainic acid-evoked neurodegeneration in the rat brain. Neurosci. Lett. 326, 129–132.

Bak, L.K., Schousboe, A., Waagepetersen, H.S., 2006. The glutamate/GABA-glutamine cycle: aspects of transport, neurotransmitter homeostasis and ammonia transfer. J. Neurochem. 98, 641–653.

Beniac, D.R., Wood, D.D., Palaniyar, N., Ottensmeyer, F.P., Moscarello, M.A., Harauz, G., 2000. Cryoelectron microscopy of protein–lipid complexes of human myelin basic protein charge isomers differing in degree of citrullination. J. Struct. Biol. 129, 80–95.

Boggs, J., 2006. Myelin basic protein: a multifunctional protein. Cell. Mol. Life Sci. 63, 1945–1961.

Boggs, J.M., Rangaraj, G., Koshy, K.M., Ackerley, C., Wood, D.D., Moscarello, M.A., 1999. Highly deiminated isoform of myelin basic protein from multiple sclerosis brain causes fragmentation of lipid vesicles. J. Neurosci. Res. 57, 529–535.

Brady, G.W., Murthy, N.S., Fein, D.B., Wood, D., Moscarello, M., 1981. The effect of basic myelin protein on multilayer membrane formation. Biophys. J. 34, 345–350.

Calabrese, R., Zampieri, M., Mechelli, R., Annibali, V., Guastafierro, T., Ciccarone, F., Coarelli, G., Umeton, R., Salvetti, M., Caiafa, P., 2012. Methylation-dependent PAD2 upregulation in multiple sclerosis peripheral blood. Mult. Scler. J. 18, 299–304.

Cao, L., Goodin, R., Wood, D., Moscarello, M.A., Whitaker, J.N., 1999. Rapid release and unusual stability of immunodominant peptide 45–89 from citrullinated myelin basic protein. Biochemistry 38, 6157–6163.

D'Souza, C.A., Moscarello, M.A., 2006. Differences in susceptibility of MBP charge isomers to digestion by stromelysin-1 (MMP-3) and release of an immunodominant epitope. Neurochem. Res. 31, 1045–1054.

Duchen, M.R., 2004. Mitochondria and calcium: from cell signalling to cell death. J. Physiol. Lond. 529, 57–68.

Ferguson, C.J., Lenk, G.M., Meisler, M.H., 2009. Defective autophagy in neurons and astrocytes from mice deficient in PI (3, 5) P2. Hum. Mol. Genet. 18, 4868–4878.

Ferrari-Lacraz, S., Sebbag, M., Chicheportiche, R., Foulquier, C., Serre, G., Dayer, J.M., 2010. Upon contact with stimulated T cells, expression of peptidylarginine deiminase 2 and 4 is upregulated in human monocytes. Ann. Rheum. Dis. 69, A2.

Frischer, J.M., Bramow, S., Dal-Bianco, A., Lucchinetti, C.F., Rauschka, H., Schmidbauer, M., Laursen, H., Sorensen, P.S., Lassmann, H., 2009. The relation between inflammation and neurodegeneration in multiple sclerosis brains. Brain 132, 1175–1189.

Harauz, G., Musse, A.A., 2007. A tale of two citrullines—structural and functional aspects of myelin basic protein deimination in health and disease. Neurochem. Res. 32, 137–158.

Harauz, G., Ishiyama, N., Hill, C., Bates, I.R., Libich, D.S., 2004. Myelin basic protein—diverse conformational states of an intrinsically unstructured protein and its roles in myelin assembly and multiple sclerosis. Micron 35, 503–542.

Hill, J.A., Southwood, S., Sette, A., Jevnikar, A.M., Bell, D.A., Cairns, E., 2003. Cutting edge: the conversion of arginine to citrulline allows for a high-affinity peptide interaction with the rheumatoid arthritis-associated HLA-DRB1* 0401 MHC class II molecule. J. Immunol. 171, 538–541.

Inagaki, M., IMakamura, Y., Takeda, M., Nishimura, T., Inagaki, N., 1994. Glial fibrillary acidic protein: dynamic property and regulation by phosphorylation. Brain Pathol. 4, 239–243.

Jack, C., Ruffini, F., Bar-Or, A., Antel, J.P., 2005. Microglia and multiple sclerosis. J. Neurosci. Res. 81, 363–373.

James, E.A., Moustakas, A.K., Bui, J., Papadopoulos, G.K., Bondinas, G., Buckner, J.H., Kwok, W.W., 2010. HLA-DR1001 presents "altered-self" peptides derived from joint-associated proteins by accepting citrulline in three of its binding pockets. Arthritis Rheum. 62, 2909–2918.

Jin, Z., Fu, Z., Troncosco, J., Everett, A.D., Van Eyk, J.E., 2013. Identification and characterization of citrulline-modified brain proteins by combining HCD and CID fragmentation. Proteomics 13, 2682–2691.

Kutzelnigg, A., Lucchinetti, C.F., Stadelmann, C., Brück, W., Rauschka, H., Bergmann, M., Schmidbauer, M., Parisi, J.E., Lassmann, H., 2005. Cortical demyelination and diffuse white matter injury in multiple sclerosis. Brain 128, 2705–2712.

Lepekhin, E.A., Eliasson, C., Berthold, C.H., Berezin, V., Bock, E., Pekny, M., 2001. Intermediate filaments regulate astrocyte motility. J. Neurochem. 79, 617–625.

Lucchinetti, C.F., Parisi, J., Bruck, W., 2005. The pathology of multiple sclerosis. Neurol. Clin. 23, 77–105.

Mastronardi, F.G., Wood, D.D., Mei, J., Raijmakers, R., Tseveleki, V., Dosch, H., Probert, L., Casaccia-Bonnefil, P., Moscarello, M.A., 2006. Increased citrullination of histone H3 in multiple sclerosis brain and animal models of demyelination: a role for tumor necrosis factor-induced peptidylarginine deiminase 4 translocation. J. Neurosci. 26, 11387–11396.

Mastronardi, F.G., Noor, A., Wood, D.D., Paton, T., Moscarello, M.A., 2007. Peptidyl argininedeiminase 2 CpG island in multiple sclerosis white matter is hypomethylated. J. Neurosci. Res. 85, 2006–2016.

Middeldorp, J., Hol, E., 2011. GFAP in health and disease. Prog. Neurobiol. 93, 421–443.

Moscarello, M.A., Wood, D.D., Ackerley, C., Boulias, C., 1994. Myelin in multiple sclerosis is developmentally immature. J. Clin. Invest. 94, 146–154.

Musse, A.A., Harauz, G., 2007. Molecular "negativity" may underlie multiple sclerosis: role of the myelin basic protein family in the pathogenesis of MS. Int. Rev. Neurobiol. 79, 149–172.

Musse, A.A., Boggs, J.M., Harauz, G., 2006. Deimination of membrane-bound myelin basic protein in multiple sclerosis exposes an immunodominant epitope. Proc. Natl. Acad. Sci. U. S. A. 103, 4422–4427.

Nicholas, A.P., Whitaker, J.N., 2002. Preparation of a monoclonal antibody to citrullinated epitopes: its characterization and some applications to immunohistochemistry in human brain. Glia 37, 328–336.

Nicholas, A.P., Sambandam, T., Echols, J.D., Tourtellotte, W.W., 2004. Increased citrullinated glial fibrillary acidic protein in secondary progressive multiple sclerosis. J. Comp. Neurol. 473, 128–136.

Nicholas, A.P., Sambandam, T., Echols, J.D., Barnum, S.R., 2005. Expression of citrullinated proteins in murine experimental autoimmune encephalomyelitis. J. Comp. Neurol. 486, 254–266.

Noseworthy, J.H., Lucchinetti, C., Rodriguez, M., Weinshenker, B.G., 2000. Multiple sclerosis. N. Engl. J. Med. 343, 938–952.

Pines, G., Danbolt, N.C., Bjørås, M., Zhang, Y., Bendahan, A., Eide, L., Koepsell, H., Storm-Mathisen, J., Seeberg, E., Kanner, B.I., 1992. Cloning and expression of a rat brain L-glutamate transporter. Nature 360, 464–467.

Potokar, M., Kreft, M., Li, L., Daniel Andersson, J., Pangršič, T., Chowdhury, H.H., Pekny, M., Zorec, R., 2007. Cytoskeleton and vesicle mobility in astrocytes. Traffic 8, 12–20.

Potokar, M., Stenovec, M., Kreft, M., Kreft, M.E., Zorec, R., 2008. Stimulation inhibits the mobility of recycling peptidergic vesicles in astrocytes. Glia 56, 135–144.

Pritzker, L.B., Joshi, S., Gowan, J.J., Harauz, G., Moscarello, M.A., 2000. Deimination of myelin basic protein. 1. Effect of deimination of arginyl residues of myelin basic protein on its structure and susceptibility to digestion by cathepsin D. Biochemistry (N. Y.) 39, 5374–5381.

Rogers, G.E., Harding, H.W.J., Llewellyn-Smith, I.J., 1977. The origin of citrulline-containing proteins in the hair follicle and the chemical nature of trichohyalin, an intracellular precursor. Biochim. Biophys. Acta Protein Struct. 495, 159–175.

Rothstein, J.D., Martin, L., Levey, A.I., Dykes-Hoberg, M., Jin, L., Wu, D., Nash, N., Kuncl, R.W., 1994. Localization of neuronal and glial glutamate transporters. Neuron 13, 713–725.

Sambandam, T., Belousova, M., Accaviti-Loper, M.A., Blanquicett, C., Guercello, V., Raijmakers, R., Nicholas, A.P., 2004. Increased peptidylarginine deiminase type II in hypoxic astrocytes. Biochem. Biophys. Res. Commun. 325, 1324–1329.

Sharma, R., Fischer, M.T., Bauer, J., Felts, P.A., Smith, K.J., Misu, T., Fujihara, K., Bradl, M., Lassmann, H., 2010. Inflammation induced by innate immunity in the central nervous system leads to primary astrocyte dysfunction followed by demyelination. Acta Neuropathol. 120, 223–236.

Shideman, C., Hu, S., Peterson, P., Thayer, S., 2006. CCL5 evokes calcium signals in microglia through a kinase-, phosphoinositide-, and nucleotide-dependent mechanism. J. Neurosci. Res. 83, 1471–1484.

Smith, K.J., 2007. Sodium channels and multiple sclerosis: roles in symptom production, damage and therapy. Brain Pathol. 17, 230–242.

Storck, T., Schulte, S., Hofmann, K., Stoffel, W., 1992. Structure, expression, and functional analysis of a Na-dependent glutamate/aspartate transporter from rat brain. Proc. Natl. Acad. Sci. 89, 10955–10959.

van der Valk, P., Amor, S., 2009. Preactive lesions in multiple sclerosis. Curr. Opin. Neurol. 22, 207–213.

Vincent, S.R., Leung, E., Watanabe, K., 1992. Immunohistochemical localization of peptidylarginine deiminase in the rat brain. J. Chem. Neuroanat. 5, 159–168.

Vossenaar, E.R., Zendman, A.J.W., van Venrooij, W.J., Pruijn, G.J.M., 2003. PAD, a growing family of citrullinating enzymes: genes, features and involvement in disease. BioEssays 25, 1106–1118.

Weksler, B.B., Subileau, E.A., Perrière, N., Charneau, P., Holloway, K., Leveque, M., Tricoire-Leignel, H., Nicotra, A., Bourdoulous, S., Turowski, P., Male, D.K., Roux, F., Greenwood, J., Romero, I.A., Couraud, P.O., 2005. Blood-brain barrier-specific properties of a human adult brain endothelial cell line. The FASEB Journal 19, 1872–1874.

Wood, D.D., Moscarello, M.A., 1989. The isolation, characterization, and lipid-aggregating properties of a citrulline containing myelin basic protein. J. Biol. Chem. 264, 5121–5127.

Wood, D.D., Bilbao, J.M., O'Connors, P., Moscarello, M.A., 1996. Acute multiple sclerosis (Marburg type) is associated with developmentally immature myelin basic protein. Ann. Neurol. 40, 18–24.